Hindawi
International Journal of Energy Research
Volume 2024, Article ID 2258610, 19 pages
https://doi.org/10.1155/2024/2258610

Research Article

Enhancing Thermal Insulation of Poly(β-Hydroxybutyrate) Composites with Charring-Foaming Agent-Coated Date Palm Wood

Amal Mlhem,[1] Basim Abu-Jdayil ,[1,2] and Muhammad Z. Iqbal [1]

[1]*Chemical & Petroleum Engineering Department, United Arab Emirates University, PO Box 15551, Al Ain, UAE*
[2]*National Water and Energy Center, United Arab Emirates University, PO Box 15551, Al Ain, UAE*

Correspondence should be addressed to Basim Abu-Jdayil; babujdayil@uaeu.ac.ae

Received 19 December 2023; Revised 8 April 2024; Accepted 15 April 2024; Published 30 April 2024

Academic Editor: Prasenjit Manna

Date palm fiber (DPF) holds great potential for composite materials, but its flammability limits its practical applications. In this study, DPF was modified using a pad-drying method to impregnate it with a 5 wt.% solution of ammonium dihydrogen phosphate (ADP). These treated fibers were then utilized to fabricate poly(β-hydroxybutyrate)- (PHB-) based composites. The resulting thermal insulators were comprehensively evaluated for their flammability, physical, mechanical, and thermophysical properties, as well as morphological and thermal stability characteristics. The findings revealed a significant reduction in flame spread and smoke suppression; however, the concentration used is not sufficient to achieve the desired rating grades. The thermal insulation capacity of the modified fiber composites was substantially enhanced, particularly with the 40% PHB/DPF-ADP composite displaying the lowest thermal conductivity at 0.0564 W/m.K. Moreover, the presence of gaps and voids at the interface led to a reduction in tensile strength to 4-7 MPa. Additionally, the modified fiber composites exhibited significantly reduced water absorption (~0.76%), attributed to the formation of a highly water-resistant substance containing a furan compound. This work provides a simple and effective approach for achieving durable flame retardancy and long-term thermal insulation performance, offering promising opportunities for the practical application of biobased PHB composites.

1. Introduction

Wood-plastic composites (WPCs) combine the characteristics of wood and plastic materials with robust dimensional stability and corrosion resistance, as well as low production and maintenance costs [1]. Currently, WPCs are used in many applications, such as household goods and building construction, among others. Nevertheless, the ease of thermal degradation, ignition, and burning of WPC restricts many of their potential applications [2]. Hence, how to improve the FR properties of WPCs must be addressed [3].

The utilization of natural fibers in biocomposites has several benefits, such as rendering them cost-effective, lightweight, and extremely abundant, in addition to being derived from natural resources [4]. The burgeoning interest in WPCs stems from their environmental, economic, and social benefits [5]. Some researchers have investigated the potential of date palm fiber- (DPF-) based composites for replacing petroleum-based thermal insulation materials such as polystyrene [4]. For example, Abu-Jdayil et al. [6] showed the thermal insulation capabilities of polystyrene-date pit composites given their thermal conductivity values that ranged from 0.0515 to 0.0562 W/m.K. In other work by Abu-Jdayil et al. [7], the addition of DPF decreased the thermal conductivity of a polylactic acid matrix to 0.0692 W/m.K at a 30 wt.% filler content. Mlhem et al. [5] reinforced the poly(β-hydroxybutyrate) matrix with DPF, and the thermal conductivity of these prepared composites varied between 0.086 and 0.11 W/m.K. Although date palm composites do feature a high insulation capacity, the flammability

of their fiber content and low thermal stability could restrict the development and use of associated biocomposites [8].

To address the flammability of wood-plastic composites, there are various strategies such as the incorporation of flame retardants (FRs) into the polymer matrix, functionalization of fiber surface, and providing fire protective surface finishing [9]. The high surface area of fibers compared to resin matrix offers the potential to locate the FRs on its surface without distributing the matrix [10]. Several flame retardants (FRs) are appropriate for use in fiber-reinforced composites [11]. The halogen-free FRs can be applied, these being the most frequently used because they release little smoke and have a low environmental impact [12, 13]. According to their chemical composition, halogen-free FRs are phosphorus-containing compounds (red phosphorus, phosphates, phosphinates, phosphites, phosphonates, phosphazene, etc.), metal hydroxides (aluminum, magnesium, calcium, zirconium, etc.), and silicon-based FRs (silicon oxide, silicate-based minerals, organic silicon-based FRs, etc.) [10]. The nitrogen–phosphorus P–N compounds have greater thermal stabilities and lower toxic smoke evolution [14]. Shukor et al. [15] reported on the effectiveness of ammonium polyphosphate (APP) in enhancing the flame retardancy properties of polylactic acid- (PLA-) kenaf fiber composites. They reported a significant increase in the limiting oxygen index (LOI) from 27.6 to 31.6 upon treatment with 20 wt.% APP. This finding shows the capability of halogen-free FRs in improving the fire resistance of PLA-kenaf fiber composites.

Ammonium dihydrogen phosphate (ADP) is a well-known flame retardant that is commonly used to prepare intumescent flame-retarding (IFR) agents, comprising acid sources, blowing agents, and carbonization agents [9]. The mechanism involves the release of phosphoric acids, and gaseous products like nitrogen, leading to the formation of a protective carbon foam [16]. Kim et al. [16] introduced ammonium polyphosphate- (APP-) based IFR to flax fiber-PP composites for investigating its influence on combustion, flammability, and mechanical properties. It was found that 15 wt.% IFR adversely affected their flame resistance and mechanical properties. The composites did not pass the vertical burning tests (UL-94), and the addition of IFR reduced the tensile and flexural strength of composites. Kim et al. [16] and Fang et al. [17] found that the flame retardant significantly mitigated the cone calorimetry results such as peak heat release rate (PHRR), total heat release (THR), and total smoke production of the composites.

Incorporating large amounts of FRs invariably degrades the filler, thereby diminishing the mechanical properties. Arao et al. [18] found that the tensile strength of polypropylene-modified wood flour with APP decreased from 50 MPa to 46 MPa and 42 MPa with an increasing concentration of the impregnating ADP solution 0, 5, and 10 wt.%, respectively. Additionally, Suardana et al. [19] reported that the strength of polypropylene-modified coconut with DAPs reduced from 12 MPa to 9 MPa. Poor compatibility between these FRs and the polymer matrix resulted in the deterioration of both tensile strength and elongation at break of the resultant wood-plastic composites [20, 21]. It is known that modifying fiber with a fire retardant reduces its tensile properties, whose use at high concentrations further deteriorates the mechanical performance of wood-plastic composites [18, 22].

Although environmentally friendly flame-retardant agents show promise, their effectiveness in improving the flame resistance of composite materials at low concentration levels is limited [9]. Kim et al. [21] produced unsaturated polyester composites reinforced with coated fiberglass at a concentration of 5, 10, or 20 wt.% ADP solution. However, both uncoated and coated fiberglass samples with a 5 wt.% ADP concentration experienced complete combustion upon initial flame exposure. As a result, subsequent UL-94 testing revealed that no ratings were achieved for these samples. In contrast, the samples were reinforced with coated fiberglass at 10 and 20 wt.% ADP, and their flames were extinguished upon the first flame application. Therefore, based on the UL-94 ratings, these unsaturated polyester composites were classified as V-1 and V-0, respectively. Furthermore, Gulati et al. [23] coated date pits with a 10 wt.% ADP solution and reinforced the linear low-density polyethylene (LLDPE) composites. Whereas the neat composite lacked a UL-94 rating given its complete burning up to the holding clamp, coating with 10 wt.% ADP augmented the rating to V-0.

Fire retardants generally have a significant influence on the water absorption of wood-plastic composites, often resulting in an increase in the water uptake of modified fiber composites [24]. Chindaprasirt et al. [25] obtained greater water adsorption values (0.64%–1.66%) of expanded polystyrene-wood flour by modifying its fiber with DAP after 24 h of testing. However, water absorption of oil palm trunk fiber modified with ADP was considerably reduced [26]. The particleboard with 0 wt.% ADP had the worst (highest) water absorption value (65.6%), with the lowest percentage obtained with 10 wt.% ADP (29.2%). Umemura et al. [27] prepared a natural wood adhesive, by mixing sucrose and ADP in various weight ratios, and these mixtures were thermally treated. They found that sucrose (water-soluble saccharides) becomes a highly water-resistant substance containing a furan ring and carbonyl group, for which ADP acts as a catalyst when heated.

Many studies extensively focus on green composites, particularly those used in construction, especially in the areas of fabrication [5, 7, 28, 29], and modification of fiber composites through treatments such as silane and alkaline [30–32]. However, there has been less attention given to investigating the effects of reinforcing fibers treated with intumescent flame retardant on the flammability and other properties of thermally insulated green composites. Therefore, this study investigates the utilization of ammonium dihydrogen phosphate (ADP, acid source, and blowing agent) and DPF (char-forming agent) for poly(β-hydroxybutyrate) (PHB) composites. Extrusion was used to melt blend each PHB-modified DPF composite, which was then molded using thermocompression and subjected to thermal annealing. The intumescent fire-retardant-treated fiber composites (PHB/DPF-ADP) were tested for flammability, physical properties, tensile, and thermophysical properties. Additionally, the samples were characterized for their thermal

stability and morphological properties with a view towards implementing sustainable development principles in the built environment.

2. Experiment

2.1. Materials. Date palm fibers (DPFs) were obtained from the farm of the United Arab Emirates University in Al Foah (Al Ain, UAE). The thermoplastic polyhydroxybutyrate (PHB) (grade ENMAT Y3000P) was supplied, in the form of semicrystalline pellets, by Tianan Biologic Materials Co. (Zhejiang, China). According to the manufacturer's specifications, the PHB has a melting temperature of 175°C. The fire retardant, ammonium dihydrogen phosphate (ADP) ($NH_4H_2PO_4$), was purchased in powder form from NICE (India).

2.2. Fiber Preparation. The raw DPFs were cleaned of dust, using deionized water, and dried in a convection oven for 24 h at 105°C. The raw DPFs were ground into powder form by mechanical grinding using a grinder (Generic, 1900-watt, China) at 28,000 rpm. Further, the fibers were sieved to ≤212 μm, and Figure 1 shows the cumulative particle distribution for the ground DPF. Next, the powdered DPFs were dried at 80°C in the oven until the change in weight was negligible. After it cooled down to room temperature in a desiccator for two hours, the fibers were ready for coating.

2.3. Chemical Modification for Date Palm Fibers. The pad-drying process was followed in treating DPF with fire retardant (ADP). In the pad-drying process, the fiber is immersed in the bath containing a flame retardant, removing the excess solution, and then drying [33]. The powdered DPFs were further preheated in the oven at 80°C for 2 hours to improve the rewetting characteristics and to facilitate the interaction with the ADP solution [34]. Then, the dried DPFs were padded in a 5 wt.% ADP solution for 5 minutes at room temperature and filtered, following the thermotex procedure that is used for textile fabrics, elaborated by Ruszнák [35]. The ratio is 10 g fibers to 100 ml ADP solution. Then, the coated fibers were treated thermally in a convection oven at 90°C for 2 h.

2.4. Composite Fabrication. The DPFs modified with the ADP fire retardant were then used to reinforce PHB composites. This study focuses on the formulations of 20 and 40 wt.% of modified fiber-reinforced PHB. Based on previous findings [5, 27, 31], these formulations are selected because they exhibit representative behavior for composites at both low and high fiber content. The formulations were melt-blended using a lab-scale twin-screw extruder (Mini-Lab Haake, Thermo Scientific, Germany), at 175°C for 1 min, at a rotational speed of 200 rpm. The resulting mixture was thermally pressed using compression molding (Auto Four-3015 Carver Inc., USA), after which the produced samples were annealed at 120°C for 1 h in an oven (forced convection oven-Lab Companion).

Four molds from stainless-steel material were used to prepare composite samples having different shapes and dimensions (Figure 2). Under the same controlled conditions, the

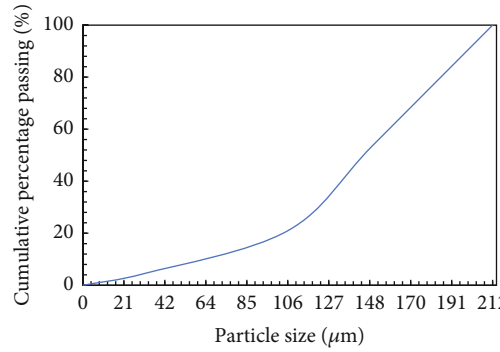

Figure 1: Cumulative particle distribution curve for date palm fiber (DPF).

Figure 2: The four molds used in preparing the composite samples.

plate-, bar-, and dog bone-shaped composites were prepared, while cylindrical samples were fabricated another way. The dimensions of plate specimens (11 mm × 11 mm × 3 mm) followed the ASTM C518 [36]. These plate-shaped samples were tested for thermal conductivity, from which fragments were cut to conduct characterization tests. The dog bone-shaped (62 mm × 14 mm × 3 mm) samples were used for tensile strength and SEM tests, and the bar-shaped samples (100 mm × 4 mm × 3 mm) were used for the UL-94 vertical burning test. The cylindrical samples (25.7 mm × 12.8 mm), whose fabrication was based on ASTM-D570 [37], were used for carrying out the density and water absorption tests.

All samples were prepared under the same conditions (pressure, temperature, and duration), except for the cylindrical samples (differing temperature and duration). The plate, dog bone-, and bar-shaped composites were made using a three-segment heating cycle: samples were pressed at 500 kgf and melted at 177°C for 4.5 min (step 1); each sample was then melted at 180°C and pressed at 520 kgf for 4 min (step 2); finally, the pressure was increased to 3000 kgf at 100°C for 3.3 min (step 3). Furthermore, under the same pressure conditions, the cylindrical composite samples were obtained. For these, however, a temperature of 190°C was applied for 23 min (step 1). Then, each sample was then melted under the same temperature for 16 min (step 2). The cycle was completed by melting the samples at 100°C for 11 min (step 3). Table 1 gives the formulations of the composites used in this study. The three proportions

Table 1: Nomenclature used for raw and modified DPF-reinforced PHB composites.

Code	DPF (wt.%)	PHB (wt.%)	Samples
Neat PHB	00	100	Poly(β-hydroxybutyrate)
20% PHB-DPF	20	80	Uncoated fiber-reinforced PHB
20% PHB/DPF-ADP	20	80	Coated fiber-reinforced PHB
40% PHB-DPF	40	60	Uncoated fiber-reinforced PHB
40% PHB/DPF-ADP	40	60	Coated fiber-reinforced PHB

of modified DPF with ADP were used to prepare the PHB composites through melt blending, thermocompression molding, and annealing processes. The resulting thermal insulators were comprehensively evaluated for their flammability, physical, mechanical, and thermophysical properties, as well as morphological and thermal stability characteristics. In this study, a range of 3 to 5 samples for each formulation was prepared for testing, and their standard deviation (S.D.) was calculated and presented using Excel.

2.5. Measurements. The micro structure of modified fibers and its composites was examined using scanning electron microscopy (SEM) (5000 NeoScope, JOEL, Tokyo, Japan). Before their measurement, each sample was prepared by gold sputtering it directly. The SEM images of samples were obtained under observation conditions of 10, 50, and 100 μm.

Fourier-transform infrared (FTIR) spectra in the range of 400–4000 cm^{-1} were recorded on a Jasco FTIR spectrometer. The fibers in powdered form were mixed with a potassium bromide (KBr) powder and compressed into a disc. Small portions were cut from composite samples for testing. The spectra were recorded at a resolution of 4 cm^{-1} and 32 scanning times and subjected to baseline correction.

Thermal properties of the PHB composites were characterized by differential scanning calorimetry (model 25DSC, TA Instruments, Delaware, USA). Prior to these measurements, each sample was heated from –10°C to 200°C at a rate of 5°C/min. At the same rate, the sample was held annealed at 120°C for 1 hour; then, it was cooled down to –10°C after which it was reheated at 200°C at 5°C/min. All measurements were carried out under the nitrogen flow at a rate of 50 ml/min. The melting temperature (T_m) and melting enthalpy (ΔH_m) were determined from the DSC curves. The degree of crystallization (X_c) was calculated this way:

$$X_C = \frac{\Delta H_m}{\Delta H_{m,100\%} \cdot \varphi_{\mathrm{PHB}}}, \quad (1)$$

where $\Delta H_{m,100\%}$ is the theoretical melting enthalpy of a 100% crystalline PHB (146 J/g) [38], ΔH_m is the melting enthalpy of a composite, and φ_{PHB} is the PHB mass fraction in each composite (Table 1).

The density of cylindrical samples was determined for three replicates, as the mass of the composite to its volume ratio, by following ASTM-C134 [39]. A digital analytical balance (OHAUS PR124, China) was used to weigh each sample (±0.0001 g), and a vernier caliper was used to measure their dimensions.

A FOX-200 heat flow meter (TA Instruments-Laser-Comp, MA, USA), equipped with a cooling apparatus to control the temperature by Thermo Cube (Solid State Cooling System, NY, USA), was used to measure thermal conductivity. These measurements were taken at room temperature once a steady state was achieved and by following ASTM C518 [36]. The average value of three replicates is presented for the plate samples. The heat flow meter is presented in Figure 3.

Thermal diffusivity (α) was calculated by using the directly measured thermal conductivity (k), density (ρ), and specific heat capacity (C_p), as follows:

$$\alpha = \frac{k}{\rho C_p}, \quad (2)$$

in which the specific heat capacity C_p was tested thrice using the DSC for each formulation. The experiment used a heating rate of 3°C/min over a temperature range of 5–60°C, in accordance with the modulated DSC. The measurements obtained at 25°C are reported in this paper.

Tensile properties (strength, strain, and Young's modulus) were evaluated with a testing machine (Shimadzu's AG-X) as seen in Figure 4, using a crosshead speed of 5 mm/min following ASTM D3039 [40]. The dog bone-shaped samples (in triplicate) were at room temperature.

The water absorption test for PHB/DPF-ADP composites was carried out in accordance with ASTM-D570 [37] standards by soaking in distilled water at 25°C and 50°C for 48 hours. The cylindrical-shaped composites were tested in triplicate. They were periodically removed from the water bath and weighed after wiping their surfaces with tissue paper. Their water absorption percentage (M_t) was calculated this way:

$$M_t = \frac{W_w - W_d}{W_d} \times 100, \quad (3)$$

where W_d is the weight of the dry sample (g) and W_w is that of the wet sample (g) after immersion.

A thermogravimetric analysis (TGA) was used to conduct the pyrolysis tests (TGA Q500, TA Instruments, USA). To investigate the thermal oxidation resistance of each composite, about 7.0 ± 2.0 mg of mass was placed on the TGA pan and heated at a rate of 10°C/min. The first

Figure 3: Heat flow meter to measure thermal conductivity.

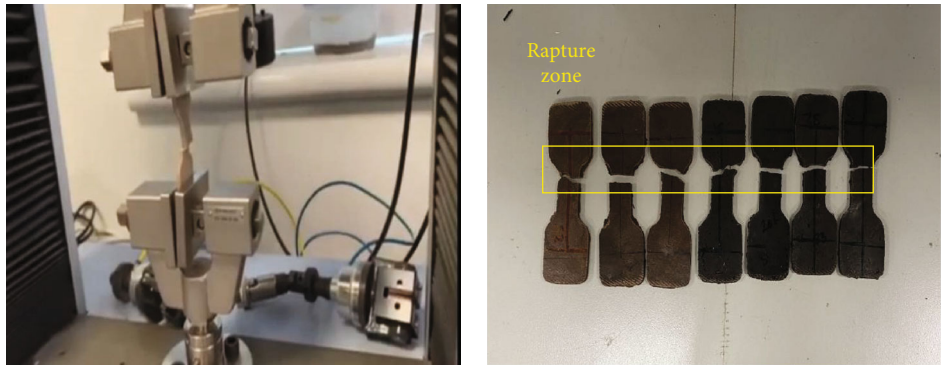

(a) (b)

Figure 4: Tensile test: (a) tensile machine and (b) tested tensile samples with their rapture zone.

Table 2: Burning criteria for UL-94 vertical rating.

Test criteria	UL 94 V rating		
	V-0	V-1	V-2
Burning time (s) of each individual test composite (after T_1 and T_2)	10≥	30≥	30≥
Second flam application (s), after burning and afterglow times	30≥	30≥	60≥
Ignition of surgical cotton due to melt dripping	No	No	Yes
Composites completely burned up to the holding clamp	No	No	Yes

derivative of the thermogram (DTG) was obtained using Pyris software.

UL-94 vertical burning test was conducted for five bar-shaped samples according to UL94 standards, by using a UL 94 vertical burning test apparatus and following ASTM 3801. Each bar was suspended vertically over surgical cotton and ignited with a Bunsen burner, with the lower end of the bar exposed to the flame for 10 s. The tested samples were classified into three rating categories based on the summation of flame times of the first and the second timed applications ($T_1 + T_2$), as presented in Table 2. The ratings are V-0 (i.e., self-extinguishing capability within 10 sec without melt dripping), V-1 (self-extinguishing capability within 30 sec without melt dripping), and V-2 (self-extinguishing capability within 30 sec with melt dripping).

3. Results and Discussion

3.1. Scanning Electron Microscopy. Figure 5 shows the scanning electron microscopy (SEM) micrographs of neat PHB, raw DPF, modified fiber, and the tensile fracture of their composite sample. The fracture surface of the neat PHB specimen has no visible gaps or weaknesses as depicted in Figure 5(a) [5]. The raw DPF has a cylindrical shape and traces of impurities along its longitudinal surface (Figure 5(b)). This surface structure is similar to that of sisal fiber [41]. The surface of the coated DPF was partly peeled off and had an inhomogeneous surface structure (red circle), as shown in Figures 5(c) and 5(d). Moreover, this inhomogeneity was due to the agglomeration of the fire retardant on the DPF surface. Inorganic FRs reportedly have a strong surface polarity; hence, they are easily agglomerated [42]. A similar observation was reported by Bachtiar et al. [43], in that APP increased the surface roughness of flax fiber, subsequently reducing the contact area between the epoxy resin and the modified flax fiber. Figures 5(e) and 5(f) show that a 40% PHB–DPF composite has pull-out and void content and microcrack within the sample. From Figures 5(g) and 5(h), it is evident that the fiber pull-out seems higher for PHB/DPF-ADP composites than for PHB-DPF composite.

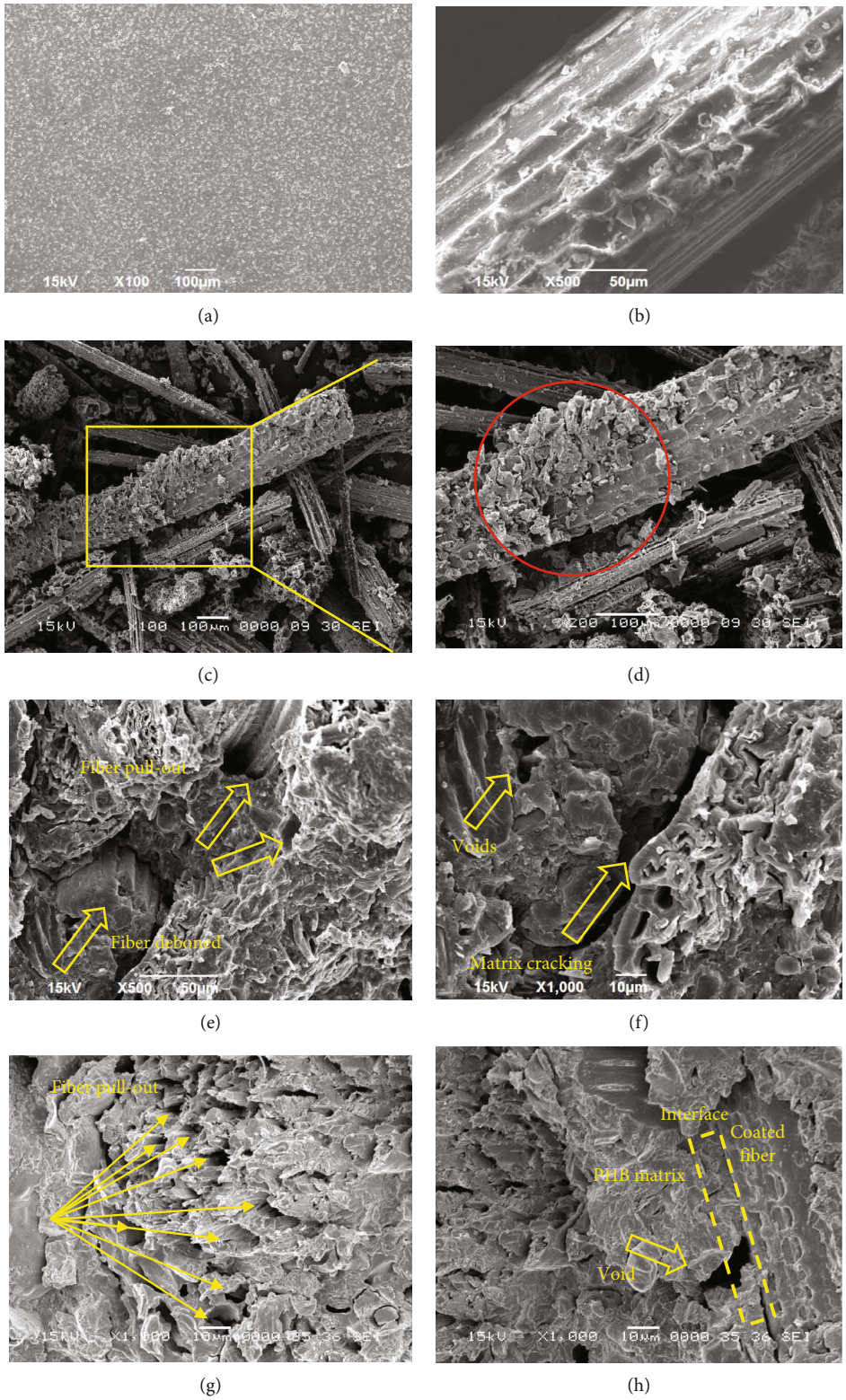

Figure 5: SEM results of (a) neat PHB, (b) uncoated date palm fiber, (c, d) coated fiber with ammonium dihydrogen phosphate, (e, f) 40% PHB-DPF, and (g, h) 40% PHB/DPF-ADP.

A similar observation was obtained by Niu et al. [44] on the surface of the PLA modified with APP-bamboo fiber; this was caused by the pulling out of modified bamboo fiber due to its weak interface adhesion with coated PLA. The more pull-out indicates that the interfacial adhesion is poor between the modified fiber and the matrix [45]. That result corroborated the low interfacial bonding found here between the modified DPF and PHB. Figure 5(h) shows an

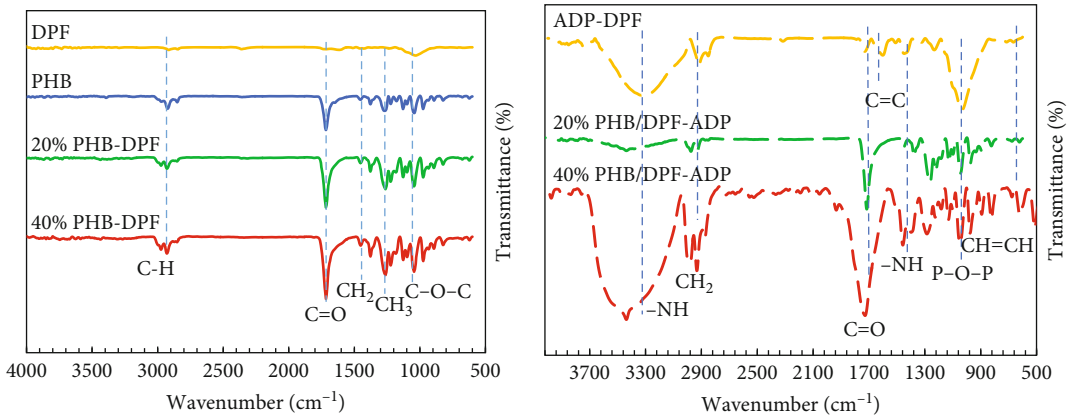

Figure 6: FTIR spectra of (a) raw and (b) modified DPFs, with their composites.

Table 3: FTIR bands observed for the samples.

Band position in this work (cm^{-1})	Wavenumber (cm^{-1})	Functional groups	References
3334	3343	Stretching of –NH	Prabhakar et al. [50]
2915–2849	2980–2800	Symmetric and asymmetric stretching of CH_2	Zhou et al. [56] Chung et al. [46]
1450	1430	Vibration of NH ($NH4^+$)	Prabhakar et al. [50]
1715,1718	1764	Stretching vibration of C=O	Ghosh et al. [47]
1600	1510–1515	Stretching of C=C of the furan ring	Komariah et al. [51]
1300–1000	1300–1000	Symmetric and asymmetric stretching of C–O	Guimarães et al. [48]
1250	1260	Stretching vibration of P=O	Prabhakar et al. [50]
1077	1077	Stretching vibration of P–O–P	Prabhakar et al. [50]
712	780	CH=CH of the furan ring	Komariah et al. [51]

obvious void between the fibers and PHB (yellow arrow), indicative of weak interfacial adhesion between PHB and coated DPF.

3.2. Fourier-Transform Infrared (FTIR) Spectroscopy. The functional group analyses of uncoated and ADP fibers and their composites were studied using FTIR spectroscopy, with their resulting spectra shown in Figure 6. Table 3 lists the FTIR peak locations and their corresponding functional groups.

The DPFs and its composite displayed extra peaks at 2915 cm^{-1} and 2849 cm^{-1}, which corresponded to the asymmetric and symmetric stretching of methylene ($-CH_2-$) groups in long alkyl chains due to the presence of waxes [5, 46]. At 1715 cm^{-1}, the stretching vibration of the acetyl group or ester was related to the carbonyl group C=O in hemicellulose [47]. The peaks in region between 1300 cm^{-1} and 1000 cm^{-1} are related to the stretching of C–O bonds, these being characteristic of alcohol, carboxylic acids, ester, or ether functional groups, present in fiber [48].

Regarding the ADP system, the –NH stretching band of primary amines in the ADP structure was situated at 3334 cm^{-1}. Wang et al. [49] found that the polyurethane-modified wood flour composites featured a peak at 3343 cm^{-1} that was related to the stretching of –NH in APP [50]. Moreover, it was reported that the –NH peak exhibits a characteristic distinct from the –OH peak, in being noticeably sharper [49]. The intensity of peak 1718 cm^{-1} can be attributed to the carbonyl group (C=O), while 1600 cm^{-1} is ascribed to C=C, and 712 cm^{-1} to CH=CH in the furan ring [51, 52]. The addition of ADP onto DPFs under the heat treatment effect produced a high water-resistant substance resembling a furan product [52]. It is worth emphasizing that furanic products are produced under the effect of thermal curing, and these products are considered water resistant [19, 52, 53].

The intensity of the carbonyl group (C=O) was greater relative to the uncoated fiber composites This increase is attributable to the esterification of phosphoric acid with the hydroxyl group in the fiber, leading to augmented char formation, which enhances the flame retardancy of the material [19]. The band at 1600 cm^{-1} disappeared because of a condensed carbon shell generated on the surface of the PHB/DPF-ADP composite; this leads to low smoke production during burning [54]. The peaks at 1450 cm^{-1}, 1250 cm^{-1}, and 1077 cm^{-1}, respectively, corresponded to the stretching vibration of NH ($NH4^+$), P=O, and P–O–P in ADP [50, 55]. Putu et al. [19] reported that the DAP fire retardant can decompose at 160°C into ammonia and phosphoric acid. The fiber's hydroxyl groups would react with

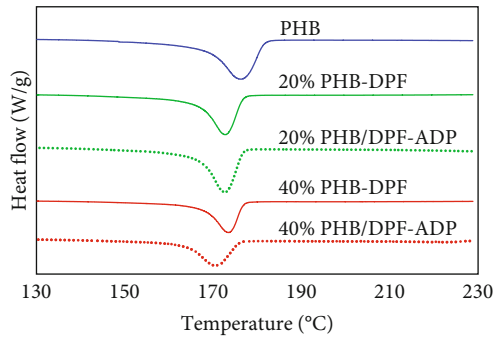

Figure 7: DSC results obtained from 2nd heating cycle for PHB, PHB-DPF, and PHB/DPF-ADP composites.

Table 4: DSC results for PHB, neat composites, and modified fiber composites.

Sample	ΔH_m (J/g)	T_m (°C)	X_c (%)
PHB	93.99	176.3	64.4
20% PHB-DPF	79.71	172.8	68.2
20% PHB/DPF-ADP	83.25	173	71.2
40% PHB-DPF	62.44	171.5	71.3
40% PHB/DPF-ADP	54.79	170.7	62.5

phosphoric acid to form phosphorus esters (P–O–P), via phosphorylation, such that phosphate groups replace OH.

3.3. Differential Scanning Calorimetry. DSC was used to evaluate the thermal properties of neat PHB, PHB-DPF, and PHB/DPF-ADP composites, whose results are shown in Figure 7 and Table 4. When the fiber content is low, the PHB/DPF-ADP composite has a value close to the melting enthalpy and the degree of crystallinity of neat PHB-DPF composites. Adding ADP increased the melting enthalpy from 79.71 J/g to 83.25 J/g. Accordingly, to melt the PHB/DFP-ADP composites, a higher energy level is required than that by the neat composite [57]. Similarly, X_c rose from 68.2% to 71.2%. This behavior suggests that reinforcement has a nucleating effect that drove a marginal increase in the degree of crystallization [58].

However, when the fiber content is high, both the heating enthalpy and degree of crystallinity of the PHB/DPF-ADP composite were significantly reduced. The ΔH_m of PHB/DPF-ADP was 54.79 J/g, being much lower than that of the PHB-DPF composite (71.3 J/g). Other research has shown that fire retardants absorbed more heat energy in the melting of composites [59]. Concerning X_C, for PHB/DPF-ADP, it was reduced to 62.5%, due to the presence of the FR that obstructs crystallization [59]. Work by Pham et al. [59] demonstrated that, after modifying the wood flour with DAP and aluminum diethyl phosphinate FRs, the ΔH_m was reduced from 51 J/g to 32 and 46 J/g, respectively. This reduction could be attributed to the presence of voids in the composite and the low compatibility of the charred layer with the matrix. On the other hand, despite the coated DPF, the melting temperature of composites did not change significantly, ranging narrowly between 173°C and 170.7°C. A similar observation was made by Zhao et al. [58], where the melting temperature hardly changed, from 149°C to 150°C, for polypropylene-coated hemp fiber composites with APP. The low dispersion of modified DPF in the PHB matrix, along with the pronounced interaction between coated fiber particles, marginally increases the PHB/DPF-ADP composite's melting point [57].

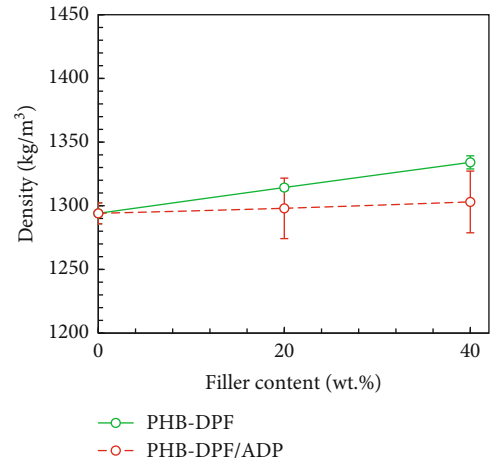

Figure 8: Experimental density of PHB-DPF and PHB/DPF-ADP composites.

3.4. Density. To investigate the effect of ADP on PHB-DPF composites, the density results of PHB/DFP-ADP are shown in Figure 8 and compared with those of the neat PHB-DPF composite. The density of PHB-DPF varied from 1314 to 1334 kg/m^3, with filler proportions of 20 and 40 wt.%, respectively. On the other hand, the PHB/DFP-ADP composite is less dense than either neat composite with values of 1298–1303 kg/m^3. This reduction in density values could be explained by ADP acting as a blowing agent, producing a low-density material [13]. The obtained density values here exceed those of foam composites like epoxy-silylated pine wood fiber (690–750 kg/m^3) and other natural fiber-based composites: polyurethane-silylated sugar palm fiber (1070–1130 kg/m^3), polystyrene-DPF (972–882 kg/m^3) [60], and lower than PLA-silylated DPF (1220–1187 kg/m^3) [7].

3.5. Thermal Conductivity. Thermal conductivity is a critical property of thermal insulating materials used in buildings, and it varies among different materials [61]. Figure 9(a) shows the thermal conductivity values of the modified fiber composites, which ranged narrowly between 0.0574 and 0.0564 W/m.K. The obtained values are evidently lower than those found for the neat composites (0.0916–0.105 W/m.K). The significant increase in thermal insulation capacity is attributed to the formation of charred layer during compression molding under the influence of heat. This charred layer is firmly attached on the DPF surface and acts as a thermal barrier by restraining the diffusion of heat [13, 21, 62].

The obtained values are slightly greater than those of conventional heat insulation materials, such as expanded polystyrene (0.030–0.040 W/m.K) [63], extruded polystyrene

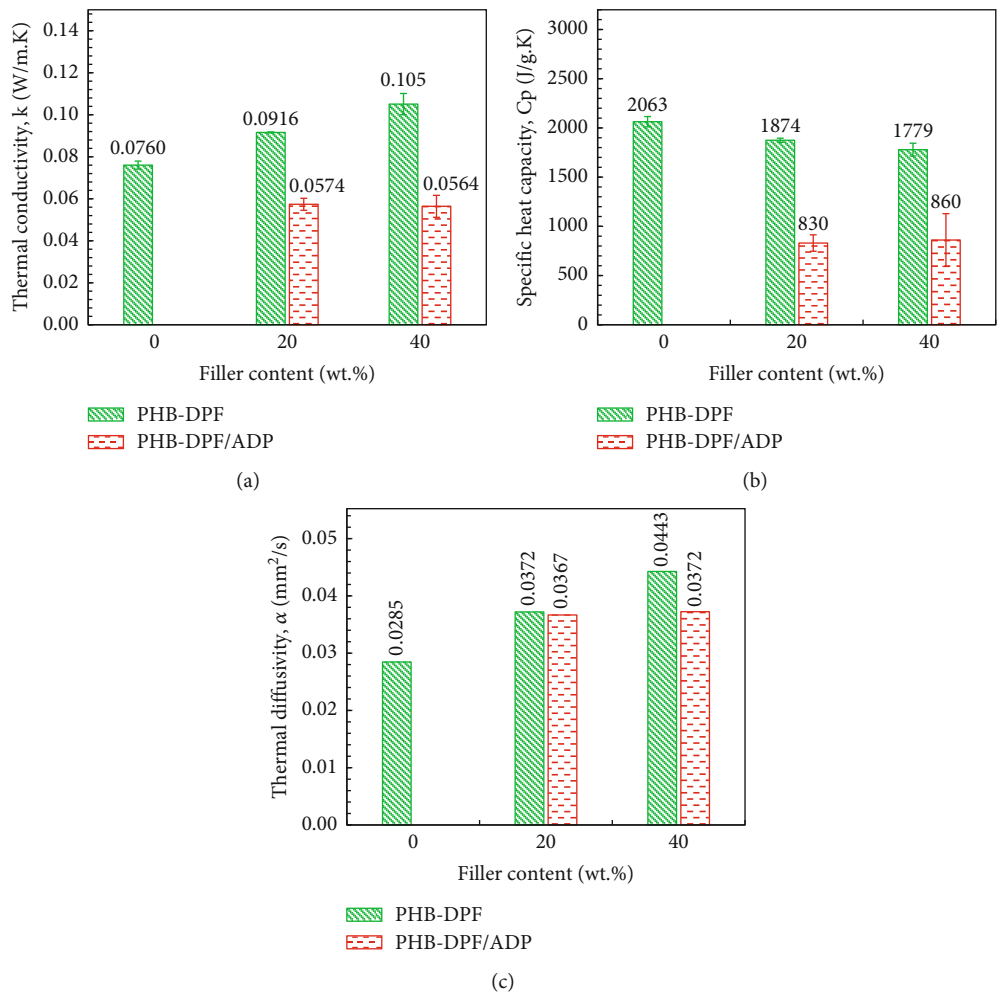

Figure 9: Thermophysical properties: (a) thermal conductivity k, (b) specific heat capacity C_p, and (c) thermal diffusivity α of PHB/DPF-ADP composites.

(0.025–0.035 W/m.K) [63], and polyurethane (0.022–0.040 W/m.K) [64]. Furthermore, the developed composites have lower thermal conductivity values than do natural fiber-based composites like polylactic acid-silylated DPF (0.087 to 1.050 W/m.K) [30], polystyrene-DPF (0.118–0.141 W/m.K) [60], and PLA modified with APP-bamboo fiber (0.35 W/m.K) [44].

3.6. Specific Heat Capacity and Thermal Diffusivity. The specific heat capacity (C_p) and thermal diffusivity of the prepared composites are vital factors to consider as well in evaluating their overall thermal performance. As Figure 9(b) shows, the C_p of PHB/DPF-ADP was 830 to 860 J/kg. K, being lower than that of neat composites (1874–1779 J/kg. K). This lower specific heat capacity is due to the voids inside the composites resulted from the expanded charred layer. The obtained values of C_p were lower than those of many commercial materials, for example, fiberglass (900 J/kg. K) [65], expanded polystyrene (1250 J/kg. K), phenolic foam (1300–1400 J/kg. K), and close from the stone wall (800–1000 J/kg. K) [64].

The thermal diffusivity was calculated using equation (2); it measures the rate of heat propagation through a material [66]. In Figure 9(c), the PHB-DPF composites exhibited very low thermal diffusivity values (0.0372–0.0443 mm^2/s). However, the values were slightly lower for PHB/DPF-ADP composites than neat composites, as the values varied from 0.0367 mm^2/s to 0.0372 mm^2/s. This is due to the presence of more voids in the coated fiber composites, resulting in lower thermal diffusivity [67]. Further, the thermal diffusivity of the modified fiber composites is much lower than that of traditional insulators like expanded polystyrene (0.544–0.638 mm^2/s) and extruded polystyrene (0.385–0.467 mm^2/s) [4]. Moreover, the low thermal diffusivity of PHB/DPF-ADP composites confers a crucial advantage to this material: it minimizes heat flow inside a building in summer, thereby enhancing the net thermal efficiency of buildings [68].

3.7. Tensile Properties. Tensile strength is a robust indicator of interfacial bonding between fibers and their matrix [69]. Figure 10 depicts the influence of ADP upon tensile properties of neat composites. Evidently, the tensile strength of the

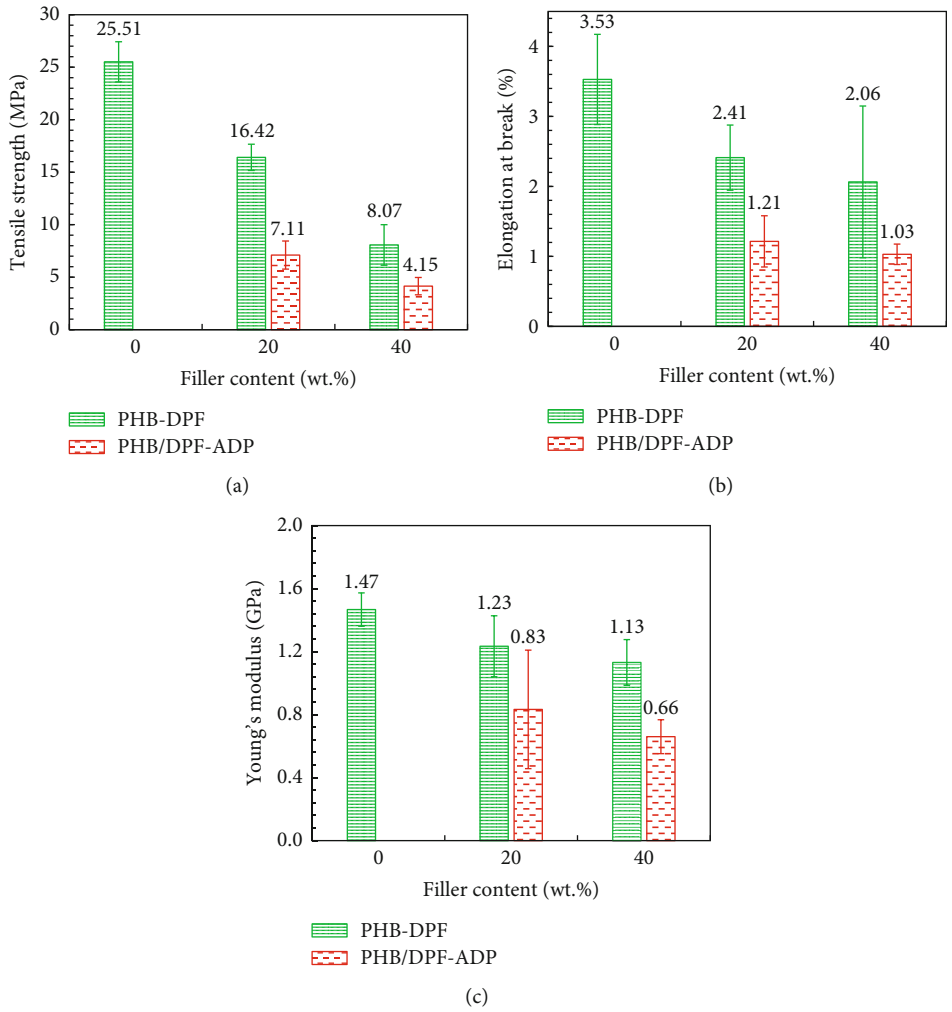

Figure 10: Tensile properties for PHB/DPF-ADP composites: (a) tensile strength, (b) elongation at break, and (c) Young's modulus.

PHB/DPF-ADP composite is weakened by an increased filler content, which is ascribed to poor adhesion between coated fibers and the matrix [19].

The tensile strength dropped from 7.11 MPa to 4.15 MPa upon incorporating 20 and 40 wt.% proportions of modified DPF, respectively. Arao et al. [18] also found that APP reduced the tensile strength of polypropylene-modified wood flour from 50 to 42 MPa. Additionally, Suardana et al. [19] reported tensile strength falling from 12 MPa to 9 MPa for a polypropylene-modified coconut with DAPs. Although incorporating ADP reduced the tensile strength, under tensile force, the prepared composites nonetheless outperformed polyurethane foam (0.110 MPa) [70], concrete (2.77 MPa) [71], extruded polystyrene (0.35 MPa), and expanded polystyrene (0.52 MPa) [72].

It is clear from Figure 10(b) that tensile strain decreases as the fiber loading increases. The strain values for the modified fiber composites ranged between 1.21% and 1.03%, values lower than those of the neat composites (2.41%–2.06%). The obtained tensile strain values are also lower than those of many coated fiber composites, for example, PLA modified with APP-bamboo fiber (2.6%–2.1%) [44]. The weak adhesion between the fiber and matrix is attributed to the formation of voids or gaps at the interface between the coated fiber and the PHB matrix (Figure 5(h)). These voids result in lower elongation at break values compared to those of untreated fiber composites [45].

Similarly, in Figure 10(c), Young's moduli of the unmodified fiber composites are 1.23 and 1.13 GPa at a filler proportion of 20 and 40 wt.%, respectively. By contrast, the 20 and 40 wt.% of PHB/DFP-ADP attained lower tensile modulus values of 0.83 GPa and 0.66 GPa, respectively. However, Gulati et al. [23] found that Young's modulus of linear LLDPE-modified date pits with ADP composites led to an increase in the tensile modulus from 0.13 GPa to 0.16 GPa; this greater stiffness was attributed to the effective degree of bonding between the polymer matrix and inorganic filler [23]. Yet, ADP is an inorganic compound with no functional groups in its structures, while PHB is an organic polymer and their polarities are markedly different. Therefore, the bond between DPF-ADP and PHB is not as tight as that between DPF and PHB, which reduces the overall composite performance [73]. Young's modulus of PHB/DPF-ADP is comparable to that of expanded polystyrene (0.134 GPa) [74] and polyurethane (0.34–0.45 GPa) [75]. Although incorporating ADP did not enhance the tensile properties

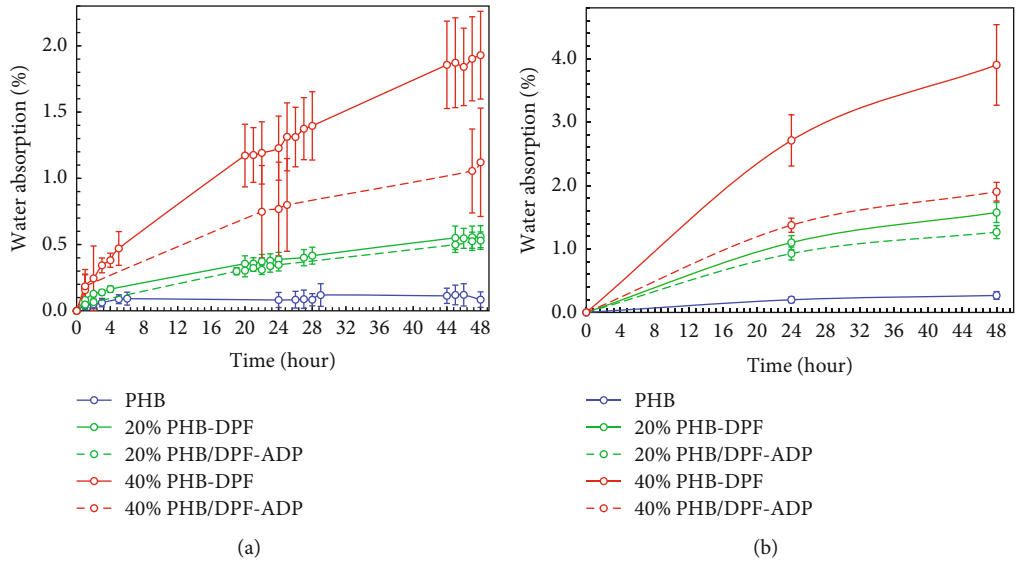

Figure 11: Water absorption of neat PHB, untreated DPF, and ADP-coated DPF composites, for (a) cold water and (b) hot water.

of composites, the results do show that these values surpass those of conventional thermal insulators. The poor compatibility between the modified DPF and PHB is due to physical interaction of the charry layer with the PHB matrix, not chemical interaction, resulting in lower tensile properties [19].

3.8. Water Absorption. Water absorption behavior was studied for the modified fiber composites and compared with those of the neat composite, and PHB matrix for 48 h, using cold (25°C) as well as hot water (50°C), as seen in Figures 11(a) and 11(b).

As Figure 11 shows, coating the fiber with ADP restricted the absorption of water to the filler surface. The PHB/DPF-ADP composites exhibited lower water absorption than did PHB-DPF composites. As shown in Figure 11(a), the composites were tested at room temperature, and it was observed that after 24 h, the 20 and 40 wt.% PHB/DPF-ADP absorbed 0.34% and 0.76% of water, respectively. After 48 hours, the reduction in water absorption was more significant for the 40% PHB/DPF-ADP composite, with the water uptake decreasing from 1.92% to 1.12% (a 42% reduction). On the other hand, Chindaprasirt et al. [25] found that the water adsorption of expanded polystyrene-wood flour increased after modifying the fiber with DAP, attaining values of 0.64–1.66% after 24 h. The PHB/DPF-ADP has a lower water absorption percentage than several treated natural fiber-based composites like epoxy-coated hemp (0.9%–1.2%) [76] and is close to that of the PLA-silylated DPFs (0.3%–0.9%) [30].

Similarly, at high water temperature (50°C) as depicted in Figure 11(b), the ADP-treated fiber samples showed a lower tendency to uptake water than those of untreated fiber samples. The 40% PHB/DFP-ADP absorbed 1.9% while the 40% PHB-DPF absorbed 3.9%. Umemura et al. [27] found that with the addition of ADP and treatment with heat, sucrose could be transformed into a high-water-resistance substance and suggested that sucrose with added ADP would likely be water resistant [77]. After heating, structures in the sucrose convert to a substance containing a furan ring. The lower water absorption may be particularly attributed to the formation of furanic compounds, as confirmed in the FTIR analysis (see Figure 6). Additionally, it is evident that the error bars increase with higher filler content. This increase is attributed to relatively low interfacial adhesion and weak dispersion of the filler in the composite, which becomes more significant at higher DPF proportions, leading to an increase in the standard deviation among the samples. Overall, it can be concluded that water resistance is another key performance advantage for PHB/DPF-ADP composites.

3.9. Thermogravimetric Analysis. The effect of flame retardant treatment on the thermal stability of both the raw and coated DPFs, as well as their composites, was analyzed using the thermogravimetric test. Additionally, the impact of the flame retardant coating on the sample's thermal decomposition during combustion and heating processes was further investigated. The TGA and DTG curves, depicted in Figures 12(a)–12(d) and 13(a)–13(c), were used to study the mass loss and thermal oxidation resistance of the samples.

As seen in Figure 12(a), the fiber was substantially decomposed in four distinctive steps. The raw DPF decomposed at temperatures of 30–153°C, due to 6% of moisture being evaporated. In the next two steps, the further declines at 160–290°C and 300–390°C are due to the pyrolysis of three major constituents of natural fibers: lignin, hemicellulose, and cellulose [69]. The neat PHB showed an initial degradation of 10% at 225.9°C, and it lost about 50% of its mass at 240°C, followed by an abrupt mass loss to reach 4.8% at 260°C. The obtained amount of residue is 1.19% at 700°C. The PHB-DPF composites had three decomposition stages corresponding to 195–290°C, 290–340°C, and 340-800°C peaking at 285°C-288°C. The decomposition at this stage is

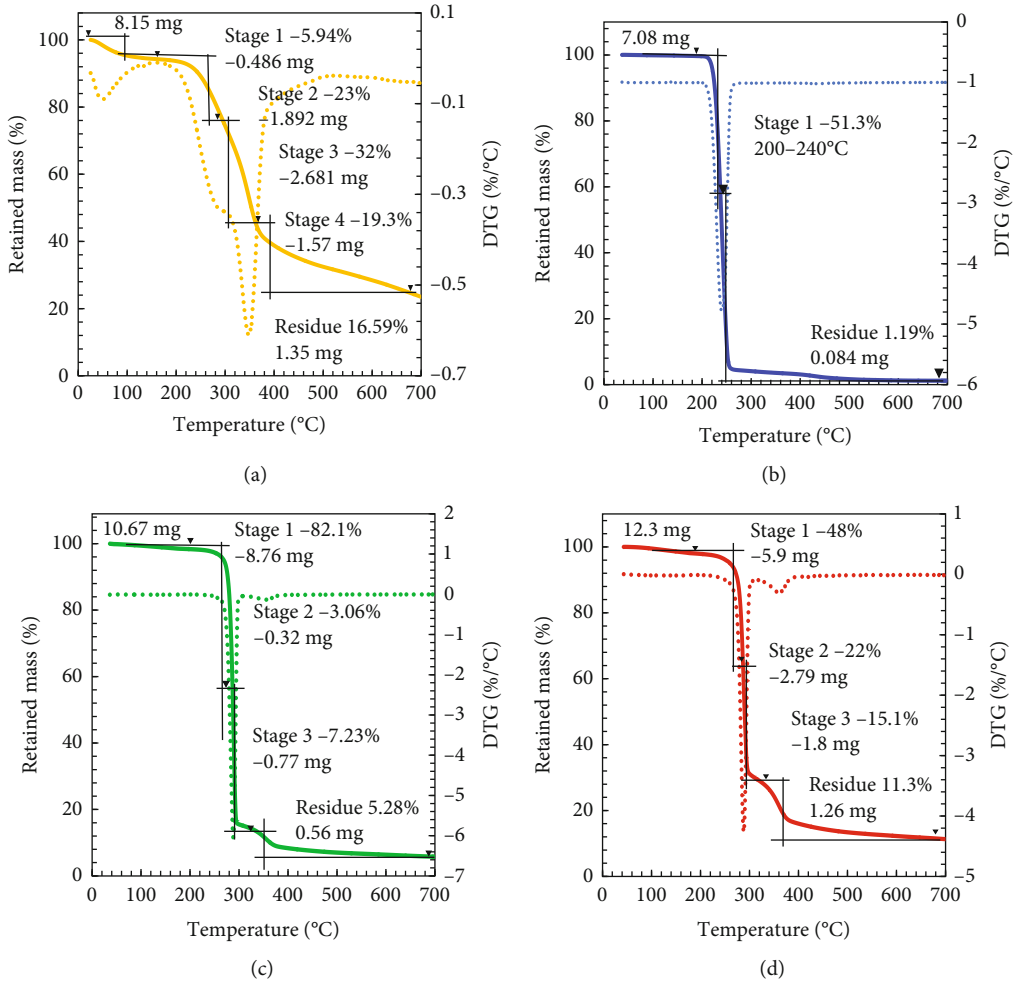

Figure 12: TGA thermograms of (a) untreated fiber, (b) neat PHB, (c) 20% PHB-DPF, and (d) 40% PHB-DPF.

attributed to the decomposition of hemicellulose, cellulose, and partially to lignin [32].

The coated fiber in Figure 13(b) has four decomposition stages, the first occurring at 30–150°C with a mass loss of 2%, which is lower than the raw DPF. The profile of the second and third steps shifted to a lower temperature of 180-260°C and 270–340°C, respectively. In this way, the inclusion of ADP changed the material's combustion pathway. The char content of coated fiber reached to 30%, a proportion considerably higher than the raw DPF (16%). Similar findings were reported for hemp fiber treated with ammonium phosphate, wherein the fire retardant promoted char formation and reduced thermal stability [78].

Regarding the composites in Figures 13(c) and 13(d), their thermal stability and char formation content were comparatively increased. At the beginning of the composite's decomposition (130-200°C), the phosphoric acid in ADP decomposes into pyrophosphoric acid and water, and then into methaphosphoric acid (HPO_3). This HPO_3 can react directly with DPF through an esterification reaction, resulting in a charry layer (carbonization) [79–81]. Simultaneously, the charry layer is expanded by the inert gases released from the ADP upon heating, forming a nonflammable and multicellular intumescent layer that covers the PHB matrix [13]. For 20% and 40% PHB/DFP-ADP composite, both exhibit a one-degradation step, at 210–300°C, with a mass loss of 63.6% and 55%, respectively. This one-degradation step is for the intumescent layer that decomposes at its maximum degradation temperature. Modifying DPF with a low concentration of ADP has a strong effect on the thermal behavior and final residues of the modified fiber composites as the highest char yield content obtained is 15.03%.

3.10. UL-94 Vertical Burning Test. The ignition resistance of composites was assessed by the UL-94 vertical burning test, and the results were classified accordingly (Table 2). Each sample was assigned to a class after measuring its duration of burning. In general, the highest rating is V-0, followed by V-1, and then V-2; the samples with a V-0 rating have the greatest flammability resistance. The flame of a sample belonging to class V-0 must self-extinguish in 10 sec or less and not glow beyond 30 sec, and no material should fall (i.e., no melt dripping). Conversely, V-2 is the most flammable [43, 82]. The fire test was applied to the PHB, neat composites, and PHB/DPF-ADP composites at a filler content of 20 and 40 wt.%, respectively (Figures 14 and 15). Their corresponding fire test results are presented in Table 5.

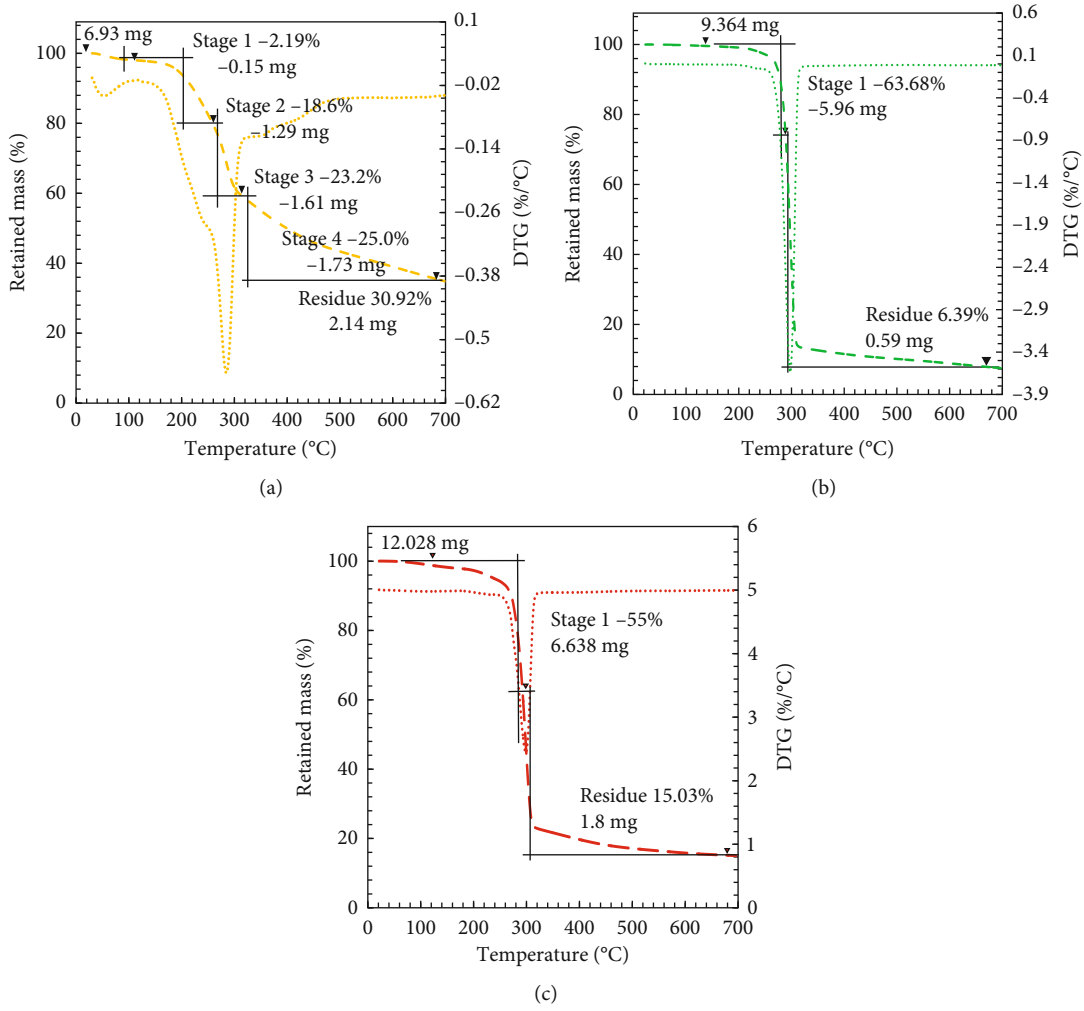

Figure 13: TGA thermograms of (a) treated fiber, (b) 20% treated fiber composite, and (c) 40% treated fiber composites.

In Figure 14(a), the fire self-extinguishing was only observed for neat PHB. After exposing the lower end of the PHB sample to the flame for 10 seconds, the flame was extinguished before 30 seconds had passed with dripping. Then, the neat PHB showed self-ignition and dripping ($T_1 \geq 50$), without applying a T_2. On the other hand, the flame had not reached the clamp (no complete combustion). Therefore, PHB had no classification (NC), due to the dripping and ignition of cotton. In Figures 14(b) and 14(c), the PHB-DPF composite was incapable of self-extinguishing (after-glowing), and its ignition time lasted more than 50 sec ($T_1 \geq 50$), without applying a second igniting (T_2). The fire reached the holding clamp with continuous melt dripping, and the surgical cotton was ignited after 50 sec from ignition. Thus, the total ignition time (T_t) for the five tested samples exceeded 250 sec ($T_t \geq 250$). Accordingly, the PHB-DPF had no classification (NC). Al Abdallah [83] obtained a similar result, where the 20% polylactic acid-DPF composite could not be classified. As for the traditional thermal insulation materials, the expanded polystyrene foam is extremely flammable, igniting easily to generate toxic black smoke during the combustion, precluding any UL-94 rating for it [84]. Similarly, the rigid polyurethane foam can also be easily ignited, and the flames can quickly spread while burning; hence, it failed to pass the vertical flame test (i.e., the UL-94 method).

The ignition resistance was determined for PHB/DPF-ADP composites, as shown in Figure 15. Although there is no obvious enhancement in fire resistance in terms of reducing the ignition time, both the flame propagation and smoldering effect are reduced. Notably, the PHB/DPF-ADP showed a lower flame spreading and burned at lower rate than did the neat composite after their ignition.

The 20 wt.% PHB/DPF-ADP started to drip continuously after 30 sec from ignition, and the flame glowed the whole sample up to the holding clamp of the holder and reached its cotton base. In general, at least 30 wt.% of the fire retardant should be incorporated into the composite to ensure an adequate self-extinguishing property and to obtain the UL-94 V-0 rating. Using that concentration or higher would be sufficient to form a charred layer that can block heat and oxygen from the combustion zone [18]. As for

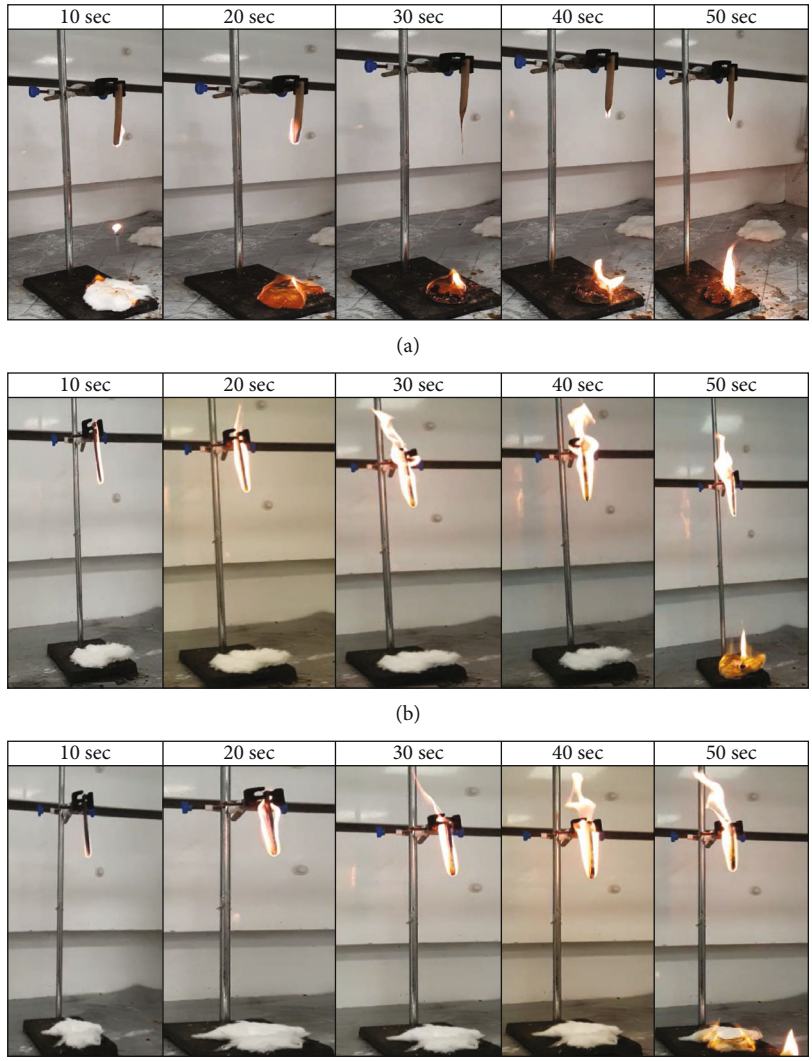

Figure 14: UL-94 vertical burning test for (a) PHB, (b) 20% PHB-DPF, and (c) 40% PHB-DPF.

the 40 wt.% PHB/DPF-ADP, the melt dripping and subsequent ignition of surgical cotton occurred after 30 sec, with no self-extinguishing observable after 60 sec. Moreover, the PHB/DPF-ADP composites underwent melt dripping 20 sec sooner than did the PHB-DPF, which can be ascribed to the low adhesion between the composite substrates. In the gas phase, the nonflammable gases derived from PHB/DPF-ADP composites diluted the concentration of combustible volatiles and oxygen and then reduced the combustion intensity. Consequently, this hindered the transfer of heat and oxygen into the interior matrix and restricted flammable volatiles from entering the flame zone. As a result, the suppression of smoke emission and the reduction of flame spreading were achieved [85, 86]. It should be stressed that no composites reinforced with fiber treated with 5 wt.% ADP met any UL-94 rating grade. Work by Lim et al. [82] showed that polypropylene-modified kenaf fiber with 30 wt.% APP had significantly reduced the combustion time, whose UL-94 rating is V-0, whereas at 10 and 20 wt.%, the composites failed to qualify for a UL-94 rating [82].

4. Impact on Composite Integrated Properties

Flame retardancy was achieved via an intumescent process; DPF serves as the charring agent, while ADP acts as the acid source and blowing agent. In Figure 16, the charred layer consists of two components: the charry layer and the intumescent layer. Initially, the charry layer forms through the dehydration of DPF, catalyzed by phosphoric acid, resulting in the formation of furan compounds, and phosphate esters. Simultaneously, ADP released gases like NH_3, causing the charred layer to expand. This expansion can result in the formation of voids within the charry layer.

According to the obtained results, the TGA test showed that the modified DPF composites started to decompose at 180-200°C. This temperature range facilitates a chemical

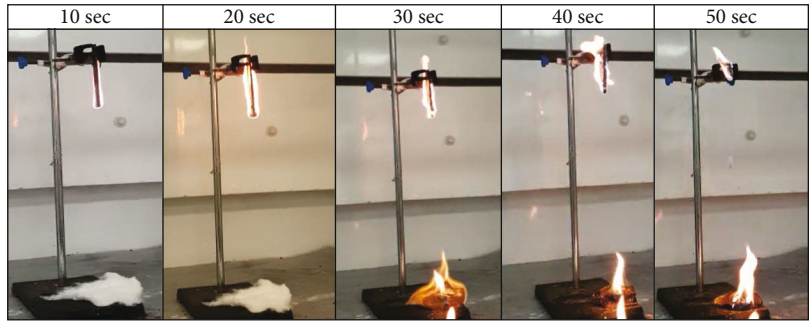

(a)

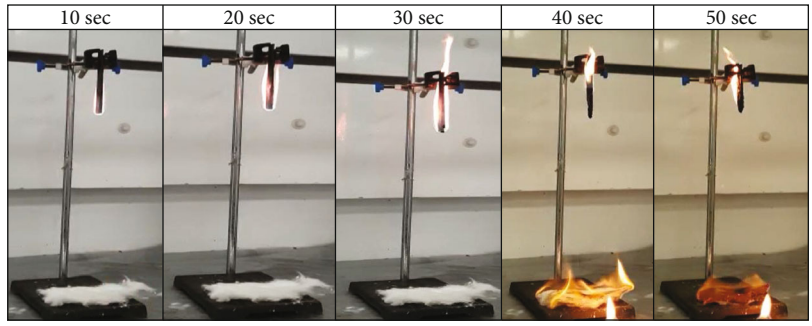

(b)

Figure 15: UL-94 vertical burning test for (a) 20% PHB/DPF-ADP and (b) 40% PHB/DPF-ADP.

Table 5: UL-94 vertical fire test results of neat composites and modified fiber composites.

Sample	T_1/T_2 (sec)	T_t (sec)	Dripping/ignition	Class
PHB	>50/-	>250	Yes/yes	NC
20% PHB-DPF	>50/-	>250	Yes/yes	NC
20% PHB/DFP-ADP	>50/-	>250	Yes/yes	NC
40% PHB-DPF	>50/-	>250	Yes/yes	NC
40% PHB/DPF-ADP	>50/-	>250	Yes/yes	NC

Note: NC: not classified by UL-94 rating.

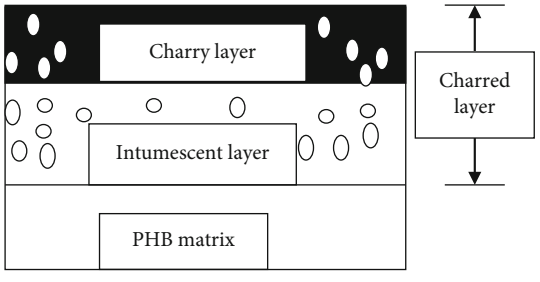

Figure 16: Intumescent flame retardant for modified PHB composites.

reaction between ADP and DPF, resulting in the phosphorylation of DPF. The composites are prepared in hot pressing around 180°C; thus, the formation of an expanded charry layer affected the properties of the composites.

The charry layer significantly reduces water absorption and increases sample volume, lowering composite density. However, the expanded charry layer reduced thermophysical properties due to the presence of voids, hindering heat flux and heat propagation time resulted in lower thermal conductivity, thermal diffusivity, and specific heat capacity. This reduction in water absorption, thermal conductivity, and diffusivity adds value to the prepared PHB-insulation composites. However, SEM confirms the poor compatibility of the charry layer with PHB due to the presence of voids, resulting in lower tensile properties. Nevertheless, these properties are still higher than those of traditional insulation materials. DSC results also confirm the presence of voids and low compatibility by the reduction in melting enthalpy. In the UL-94 vertical burning test, the intumescent layer is produced after the session of phosphate esters when the charry layer is exposed to flame or high temperature (280-300°C), which makes the charry layer to swell by ADP-released gases. The intumescent layer reduces flame propagation and smoldering by covering the PHB matrix or the condensed phase. However, the samples are not classified

by UL-94 rating, and the low concentration of ADP could not enhance the rating grades. These findings demonstrate competitive performance compared to traditional thermal insulation materials and show great potential for real-world applications.

5. Conclusion

DPF was modified using the pad-drying method for impregnation with a 5 wt.% ADP solution. The modified DPF is capable of reinforcing the PHB matrix at proportions of 20 and 40 wt.%. The results demonstrate the effectiveness of coating DPFs in enhancing the properties of PHB composites. The presence of a phosphorous ester layer (P-O-P) was confirmed through FTIR analysis. While the incorporation of ADP increases thermal stability, reduces flame spread, and suppresses smoke, it is not particularly efficient at enhancing the rating grades. The modified fiber composites exhibited a decomposition pattern with a single step, with the main weight loss occurring around 50% at 300°C. Additionally, the charred layer not only reduces the density values (1298-1303 kg/m^3) but also lowers the thermal conductivity of the composites, ranging from 0.0574 to 0.0564 W/m.K. Furthermore, the water absorption of these composites is lower (0.34%–0.76%) than that of neat composites due to the formation of a furan compound. Morphological studies of the PHB/DPF-ADP composites revealed that coating DPF caused voids or gaps in the system due to poor adhesion between the charred layer and PHB matrix. However, despite these advancements, challenges remain in achieving optimal adhesion and compatibility between modified DPFs and the PHB matrix. Consequently, there is a critical need for further improvement in the interface adhesion of ammonium dihydrogen phosphate-coated fibers. Therefore, enhancing the interface adhesion between the ammonium dihydrogen phosphate-coated fibers and the matrix is essential to improve the composites' fire performance for potential use in building construction applications.

Abbreviations

ADP: Ammonium dihydrogen phosphate
APP: Ammonium polyphosphate
DAP: Aluminum diethyl phosphinate
DPF: Date palm fiber
DSC: Differential scanning calorimetry
DTG: Derivative of the thermogram
FR: Flame retardant
FTIR: Fourier-transform infrared
LLDP: Linear low-density polyethylene
LOL: Limiting oxygen index
KBr: Potassium bromide
PHB: Poly(β-hydroxybutyrate)
PHRR: Peak heat release rate
PLA: Polylactic acid
UAE: United Arab Emirates
PVC–HDPE: Polyvinyl chloride–high-density polyethylene
SEM: Scanning electron microscopy
TGA: Thermogravimetric analysis
THR: Total heat release
WPC: Wood-plastic composites.

Data Availability

The data will be provided upon reasonable request.

Conflicts of Interest

The authors declare that they have no known competing financial interests or personal relationships that could have appeared to influence the work reported in this paper.

Acknowledgments

This work was supported by the National Water and Energy Center, United Arab Emirates University (Project # 12R122 and Project # 12R021).

References

[1] X. Zhou, Q. Fu, Z. Zhang et al., "Efficient flame-retardant hybrid coatings on wood plastic composites by layer-by-layer assembly," *Journal of Cleaner Production*, vol. 321, article 128949, 2021.

[2] K. Hu, Z. Zhao, P. Lu, S. He, C. Deng, and Y. Z. Wang, "Caffeic acid decorated ammonium polyphosphate-based flame retardant for fire safety and anti-aging of wood plastic composites," *Polymer Degradation and Stability*, vol. 209, p. 110275, 2023.

[3] N. Saba, M. Jawaid, M. T. Paridah, and O. Y. Al-othman, "A review on flammability of epoxy polymer, cellulosic and non-cellulosic fiber reinforced epoxy composites," *Polymers for Advanced Technologies*, vol. 27, no. 5, pp. 577–590, 2016.

[4] B. Abu-Jdayil, A. H. I. Mourad, A. Hussain, and H. Al Abdallah, "Thermal insulation and mechanical characteristics of polyester filled with date seed wastes," *Construction and Building Materials*, vol. 315, p. 125805, 2022.

[5] A. Mlhem, B. Abu-jdayil, T. Tong-earn, and M. Iqbal, "Sustainable heat insulation composites from date palm fibre reinforced poly (β -hydroxybutyrate)," *Journal of Building Engineering*, vol. 54, p. 104617, 2022.

[6] B. Abu-Jdayil, W. Hittini, and A. H. Mourad, "Development of date pit–polystyrene thermoplastic heat insulator material: physical and thermal properties," *International Journal of Polymeric Science*, vol. 2019, pp. 1–10, 2019.

[7] B. Abu-Jdayil, M. S. Barkhad, A.-H. I. Mourad, and M. Z. Iqbal, "Date palm wood waste-based composites for green thermal insulation boards," *Journal of Building Engineering*, vol. 43, p. 103224, 2021.

[8] L. Shumao, R. Jie, Y. Hua, and Y. Weizhong, "Influence of ammonium polyphosphate on the flame retardancy and mechanical properties of ramie fiber-reinforced poly (lactic acid) biocomposites," *Polymer International*, vol. 59, no. 2, pp. 242–248, 2010.

[9] M. Bar, R. Alagirusamy, and A. Das, "Flame retardant polymer composites," *Fibers and Polymers*, vol. 16, no. 4, pp. 705–717, 2015.

[10] D. Wang, "Flame retardancy and fire mechanical properties for natural fiber/polymer composite: A review," *Composites Part B: Engineering*, vol. 268, article 111069, 2024.

[11] B. Abu-Jdayil, "15- Application of UPR in thermal insulation systems," in *Applications of Unsaturated Polyester Resins*, S. Thomas and C. J. Chirayil, Eds., pp. 267–308, Elsevier, 2023.

[12] S. Liu, H. Wei, Y. Xiong, Y. Ding, and L. Xu, "Synthesis of a highly efficient flame retardant containing triazine and pentaerythritol phosphate groups and its intumescent flame retardancy on epoxy resin," *High Performance Polymers*, vol. 34, no. 8, pp. 889–903, 2022.

[13] X. Wang, N. Feng, S. Chang, G. Zhang, H. Li, and H. Lv, "Intumescent flame retardant TPO Composites: Flame retardant properties and morphology of the charred layer," *Journal of Applied Polymer Science*, vol. 124, no. 3, pp. 2071–2079, 2012.

[14] C. Nguyen and J. Kim, "Thermal stabilities and flame retardancies of nitrogen–phosphorus flame retardants based on bisphosphoramidates," *Polymer Degradation and Stability*, vol. 93, no. 6, pp. 1037–1043, 2008.

[15] F. Shukor, A. Hassan, S. Islam, M. Mokhtar, and M. Hasan, "Effect of ammonium polyphosphate on flame retardancy, thermal stability and mechanical properties of alkali treated kenaf fiber filled PLA biocomposites," *Materials & Design (1980-2015)*, vol. 54, pp. 425–429, 2013.

[16] N. K. Kim, R. J. T. Lin, and D. Bhattacharyya, "Flammability and mechanical behaviour of polypropylene composites filled with cellulose and protein based fibres: a comparative study," *Composites: Part A*, vol. 100, pp. 215–226, 2017.

[17] L. Fang, X. Lu, J. Zeng, Y. Chen, and Q. Tang, "Investigation of the flame-retardant and mechanical properties of bamboo fiber-reinforced polypropylene composites with melamine pyrophosphate and aluminum hypophosphite addition," *Materials*, vol. 13, no. 2, p. 479, 2020.

[18] Y. Arao, S. Nakamura, Y. Tomita, K. Takakuwa, T. Umemura, and T. Tanaka, "Improvement on fire retardancy of wood flour/polypropylene composites using various fire retardants," *Polymer Degradation and Stability*, vol. 100, pp. 79–85, 2014.

[19] N. P. G. Suardana, M. S. Ku, and J. K. Lim, "Effects of diammonium phosphate on the flammability and mechanical properties of bio-composites," *Materials and Design*, vol. 32, no. 4, pp. 1990–1999, 2011.

[20] E. N. Kalali, L. Zhang, M. E. Shabestari, J. Croyal, and D. Wang, "Flame-retardant wood polymer composites (WPCs) as potential fire safe bio-based materials for building products: preparation, flammability and mechanical properties," *Fire Safety Journal*, vol. 107, pp. 210–216, 2019.

[21] J. H. Kim, D. J. Kwon, P. S. Shin et al., "The evaluation of the interfacial and flame retardant properties of glass fiber/unsaturated polyester composites with ammonium dihydrogen phosphate," *Composites. Part B, Engineering*, vol. 167, pp. 221–230, 2019.

[22] P. Khalili, K. Y. Tshai, D. Hui, and I. Kong, "Synergistic of ammonium polyphosphate and alumina trihydrate as fire retardants for natural fiber reinforced epoxy composite," *Composites. Part B, Engineering*, vol. 114, pp. 101–110, 2017.

[23] K. Gulati, S. Lal, M. Kumar, and S. Arora, "Influence of flame retardants on LLDPE-date pit fiber composites: thermal degradation and tensile properties," *ChemistrySelect*, vol. 5, no. 29, pp. 9170–9179, 2020.

[24] K. Hämäläinen and T. Kärki, "Effects of wood flour modification on the fire retardancy of wood–plastic composites," *European Journal of Wood and Wood Products*, vol. 72, no. 6, pp. 703–711, 2014.

[25] P. Chindaprasirt, S. Hiziroglu, C. Waisurasingha, and P. Kasemsiri, "Properties of wood flour/expanded polystyrene waste composites modified with diammonium phosphate flame retardant," *Polymer Composites*, vol. 36, no. 4, pp. 604–612, 2015.

[26] R. Nur, T. Miyamoto, S. Tanaka, and K. Wiji, "High-performance binderless particleboard from the inner part of oil palm trunk by addition of ammonium dihydrogen phosphate," *Industrial Crops and Products*, vol. 141, article 111761, 2019.

[27] K. Umemura, S. Hayashi, S. Tanaka, and K. Kanayama, "Physical and chemical changes in sucrose due to the addition of ammonium dihydrogen phosphate," *Journal of The Adhesion Society of Japan*, vol. 53, no. 4, pp. 112–117, 2017.

[28] A. Mlhem, T. Teklebrhan, E. Bokuretsion, and B. Abu-Jdayil, "Development of sustainable thermal insulation based on bio-polyester filled with date pits," *Journal of Bioresources and Bioproducts*, vol. 9, no. 1, pp. 74–89, 2024.

[29] W. Hittini, B. Abu-Jdayil, and A. H. Mourad, "Development of date pit–polystyrene thermoplastic heat insulator material: mechanical properties," *Journal of Thermoplastic Composite Materials*, vol. 34, no. 4, pp. 472–489, 2021.

[30] H. Al Abdallah, B. Abu-Jdayil, and M. Z. Iqbal, "Improvement of mechanical properties and water resistance of bio-based thermal insulation material via silane treatment," *Journal of Cleaner Production*, vol. 346, article 131242, 2022.

[31] H. Al Abdallah, B. Abu-Jdayil, and M. Z. Iqbal, "The effect of alkaline treatment on poly(lactic acid)/date palm wood green composites for thermal insulation," *Polymers*, vol. 14, no. 6, p. 1143, 2022.

[32] A. Mlhem, B. Abu-jdayil, and M. Z. Iqbal, "High-performance, renewable thermal insulators based on silylated date palm fiber–reinforced poly(β-hydroxybutyrate) composites," *Developments in the Built Environment*, vol. 16, article 100240, 2023.

[33] E. Magovac and P. S. Bischof, "Non-halogen FR treatment of cellulosic textiles," *Tekstil: časopis za tekstilnu i odjevnu tehnologiju*, vol. 64, no. 9-10, pp. 298–309, 2015.

[34] A. Imtiaz, M. M. Ehsan, R. Karim, A. A. Bhuiyan, and A. Karim, "Thermochemical pretreatments to improve the fuel properties of rice husk: a review," *Renewable Energy*, vol. 215, article 118917, 2023.

[35] I. Rusznák, "Finishing of textile fabrics by the thermotex process," *Textile Research Journal*, vol. 43, no. 3, pp. 128–132, 1973.

[36] ASTM Int, *C518-15: standard test method for steady-state thermal transmission properties by means of the heat flow meter apparatus*, ASTM Int, 2015.

[37] ASTM D570, *Standard test method for water absorption of plastics*, ASTM Stand, 2014.

[38] G. J. M. de Koning, A. H. C. Scheeren, P. J. Lemstra, M. Peeters, and H. Reynaers, "Crystallization phenomena in bacterial poly[(R)-3-hydroxybutyrate]: 3. Toughening via texture changes," *Polymer*, vol. 35, pp. 4598–4605, 1994.

[39] R. Brick and I. Firebrick, "Standard test methods for size, dimensional measurements, and bulk density of," *Test*, vol. 95, pp. 1–4, 1999.

[40] ASTM, *Astm D3039/D3039M, Annu. B*, ASTM Stand, 2014.

[41] N. R. Paluvai, S. Mohanty, and S. K. Nayak, "Studies on thermal degradation and flame retardant behavior of the sisal fiber reinforced unsaturated polyester toughened epoxy nanocomposites," *Journal of Applied Polymer Science*, vol. 132, no. 24, pp. 15–17, 2015.

[42] Z. Wan, B. Zheng, X. Xie et al., "Preparation method and performance test of Evotherm pre-wet treatment aluminum hydroxide type warm-mixed flame-retardant asphalt," *Construction and Building Materials*, vol. 262, p. 120618, 2020.

[43] E. V. Bachtiar, K. Kurkowiak, L. Yan, B. Kasal, and T. Kolb, "Thermal stability, fire performance, and mechanical properties of natural fibre fabric-reinforced polymer composites with different fire retardants," *Polymers*, vol. 11, no. 4, p. 699, 2019.

[44] Q. Niu, X. Yue, Z. Guo, H. Yan, and Z. Fang, "Flame retardant bamboo fiber reinforced polylactic acid composites regulated by interfacial phosphorus-silicon aerogel," *Polymer*, vol. 252, article 124961, 2022.

[45] W. Pornwannachai, J. R. Ebdon, and B. K. Kandola, "Fire-resistant natural fibre-reinforced composites from flame retarded textiles," *Polymer Degradation and Stability*, vol. 154, pp. 115–123, 2018.

[46] C. Chung, M. Lee, and E. K. Choe, "Characterization of cotton fabric scouring by FT-IR ATR spectroscopy," *Carbohydrate Polymers*, vol. 58, no. 4, pp. 417–420, 2004.

[47] G. Ghosh, S. Saha, and S. Bhowmick, "Investigation of the effect of process parameters on fabrication of nanocrystalline cellulose from Crotalaria *juncea*," *Journal of Natural Fibers*, vol. 20, no. 1, article 2181275, 2023.

[48] T. C. Guimarães, O. D. F. M. Gomes, O. M. Oliveira de Araújo et al., "PCM-impregnated textile-reinforced cementitious composite for thermal energy storage," *Textiles*, vol. 3, no. 1, pp. 98–114, 2023.

[49] B. Wang, X. Wang, L. Zhao et al., "Effects of different types of flame-retardant treatment on the flame performance of polyurethane/wood-flour composites," *Heliyon*, vol. 9, no. 5, article e15825, 2023.

[50] M. N. Prabhakar, A. R. Shah, and J. Song, "Improved flame-retardant and tensile properties of thermoplastic starch/flax fabric green composites," *Carbohydrate Polymers*, vol. 168, pp. 201–211, 2017.

[51] R. N. Komariah, T. Miyamoto, S. S. Kusumah et al., "Effects of adding ammonium dihydrogen phosphate to a water-soluble extract of the inner part of oil palm trunk on binderless particleboard," *Bio Resources*, vol. 16, pp. 6015–6030, 2021.

[52] G. K. Dewi, R. Widyorini, and G. Lukmandaru, "Effect of ammonium dihydrogen phosphate (ADP) addition as catalyst on the curing maltodextrin adhesives properties," *Key Engineering Materials*, vol. 840, pp. 551–557, 2020.

[53] A. M. Varodi, E. Beldean, and M. C. Timar, "Furan resin as potential substitute for phenol-formaldehyde resin in plywood manufacturing," *BioResources*, vol. 14, no. 2, pp. 2727–2739, 2019.

[54] X. Long Zhao, C. Kun Chen, and X. Lei Chen, "Effects of carbon fibers on the flammability and smoke emission characteristics of halogen-free thermoplastic polyurethane/ammonium polyphosphate," *Journal of Materials Science*, vol. 51, pp. 3762–3771, 2016.

[55] D. Zhang, B. L. Williams, E. M. Becher et al., "Flame retardant and hydrophobic cotton fabrics from intumescent coatings," *Advanced Composites and Hybrid Materials*, vol. 1, no. 1, pp. 177–184, 2018.

[56] F. Zhou, G. Cheng, and B. Jiang, "Effect of silane treatment on microstructure of sisal fibers," *Applied Surface Science*, vol. 292, pp. 806–812, 2014.

[57] H. U. Zaman, R. A. Khan, and A. M. S. Chowdhury, "The improvement of physicomechanical, flame retardant, and thermal properties of lignocellulosic material filled polymer composites," *Journal of Thermoplastic Composite Materials*, vol. 36, no. 3, pp. 1034–1050, 2023.

[58] W. J. Zhao, Q. X. Hu, N. N. Zhang et al., "In situ inorganic flame retardant modified hemp and its polypropylene composites," *RSC Advances*, vol. 7, no. 51, pp. 32236–32245, 2017.

[59] L. H. Pham, L. T. Pham, D. Q. Hoang, and J. Kim, "Effective phosphorus/phosphorus-nitrogen fire retardants applied to biocomposites based on polypropylene-wood flour: flammability, thermal behavior, and mechanical properties," *Macromolecular Research*, vol. 27, no. 12, pp. 1185–1192, 2019.

[60] H. E. Benchouia, B. Guerira, M. Chikhi, H. Boussehel, and C. Tedeschi, "An experimental evaluation of a new eco-friendly insulating material based on date palm fibers and polystyrene," *Journal of Building Engineering*, vol. 65, article 105751, 2023.

[61] I. Mawardi, S. Aprilia, M. Faisal, and S. Rizal, "Investigation of thermal conductivity and physical properties of oil palm trunks/ramie fiber reinforced biopolymer hybrid composites as building bio-insulation," *Materials Today Proceedings*, vol. 60, pp. 373–377, 2022.

[62] L. Boccarusso, L. Carrino, M. Durante, A. Formisano, A. Langella, and F. M. C. Minutolo, "Hemp fabric/epoxy composites manufactured by infusion process: improvement of fire properties promoted by ammonium polyphosphate," *Composites Part B: Engineering*, vol. 89, pp. 117–126, 2016.

[63] B. Abu-Jdayil, A. H. Mourad, W. Hittini, M. Hassan, and S. Hameedi, "Traditional, state-of-the-art and renewable thermal building insulation materials: an overview," *Construction and Building Materials*, vol. 214, pp. 709–735, 2019.

[64] S. Schiavoni, F. D'Alessandro, F. Bianchi, and F. Asdrubali, "Insulation materials for the building sector: a review and comparative analysis," *Renewable and Sustainable Energy Reviews*, vol. 62, pp. 988–1011, 2016.

[65] P. Keerthan and M. Mahendran, "Thermal performance of composite panels under fire conditions using numerical studies: plasterboards, Rockwool, glass fibre and cellulose insulations," *Fire Technology*, vol. 49, no. 2, pp. 329–356, 2013.

[66] A. Djoudi, M. M. Khenfer, A. Bali, and T. Bouziani, "Effect of the addition of date palm fibers on thermal properties of plaster concrete: experimental study and modeling," *Journal of Adhesion Science and Technology*, vol. 28, no. 20, pp. 2100–2111, 2014.

[67] A. Hassn, M. Aboufoul, Y. Wu, A. Dawson, and A. Garcia, "Effect of air voids content on thermal properties of asphalt mixtures," *Construction and Building Materials*, vol. 115, pp. 327–335, 2016.

[68] E. Enríquez, V. Fuertes, M. J. Cabrera, J. Seores, D. Muñoz, and J. F. Fernández, "New strategy to mitigate urban heat island effect: energy saving by combining high albedo and low thermal diffusivity in glass ceramic materials," *Solar Energy*, vol. 149, pp. 114–124, 2017.

[69] Y. A. El-shekeil, S. M. Sapuan, K. Abdan, and E. S. Zainudin, "Influence of fiber content on the mechanical and thermal properties of kenaf fiber reinforced thermoplastic polyurethane composites," *Materials and Design*, vol. 40, pp. 299–303, 2012.

[70] S. Ma, Y. Xiao, F. Zhou et al., "Effects of novel phosphorus-nitrogen-containing DOPO derivative salts on mechanical properties, thermal stability and flame retardancy of flexible polyurethane foam," *Polymer Degradation and Stability*, vol. 177, article 109160, 2020.

[71] X. Sheng, S. Xiao, W. Zheng, H. Sun, Y. Yang, and K. Ma, "Experimental and finite element investigations on hydration heat and early cracks in massive concrete piers," *Case Studies in Construction Materials*, vol. 18, article e01926, 2023.

[72] B. Abu-Jdayil and K. Al-Malah, "Jordanian clay-based heat insulator composites: mechanical properties," *Journal of Reinforced Plastics and Composites*, vol. 27, no. 14, pp. 1559–1568, 2008.

[73] X. Jiang, P. Li, Y. Liu, Y. Yan, and P. Zhu, "Preparation and properties of APP flame-retardant ramie fabric reinforced epoxy resin composites," *Industrial Crops and Products*, vol. 197, article 116611, 2023.

[74] A. Abdel-Hakim, T. M. El-Basheer, A. M. Abd El-Aziz, and M. Afifi, "Acoustic, ultrasonic, mechanical properties and biodegradability of sawdust/recycled expanded polystyrene ecofriendly composites," *Polymer Testing*, vol. 99, article 107215, 2021.

[75] A. Shams, A. Stark, F. Hoogen, J. Hegger, and H. Schneider, "Innovative sandwich structures made of high performance concrete and foamed polyurethane," *Composite Structures*, vol. 121, pp. 271–279, 2015.

[76] S. Behera, R. K. Gautam, and S. Mohan, "Polylactic acid and polyhydroxybutyrate coating on hemp fiber: its effect on hemp fiber reinforced epoxy composites performance," *Journal of Composite Materials*, vol. 56, no. 6, pp. 929–939, 2022.

[77] R. N. Komariah, N. P. R. Krishanti, T. Yoshimura, and K. Umemura, "Characterization of Particleboard using the inner part of Oil Palm trunk (OPT) with a Bio-based Adhesive of Sucrose and ammonium Dihydrogen Phosphate (ADP)," *BioResources*, vol. 17, no. 3, pp. 5190–5206, 2022.

[78] L. Deborde, "Characterization of hemp fiber fire reaction," *Journal of Vinyl and Additive Technology*, vol. 29, no. 2, pp. 259–267, 2023.

[79] A. Pardo, J. Romero, and E. Ortiz, "Higherature behaviour of ammonium dihydrogen phosphate," *Journal of Physics: Conference Series*, vol. 935, no. 1, 2017.

[80] L. Kong, H. Guan, and X. Wang, "In situ polymerization of furfuryl alcohol with ammonium dihydrogen phosphate in poplar wood for improved dimensional stability and flame retardancy," *ACS Sustainable Chemistry & Engineering*, vol. 6, no. 3, pp. 3349–3357, 2018.

[81] B. Chol, E. Ae, Y. Jeon et al., "Improved flame-retardant properties of lyocell fiber achieved by phosphorus compound," *Materials Letters*, vol. 135, pp. 226–228, 2014.

[82] W. Y. Lim, H. E. Reeves, A. A. Somashekar, and D. Bhattacharyya, *Effects of flame retardance additives on the mechanical and fire performance of natural fibre composites*, Department of Mechanical Engineering, Auckland, New Zealand, 2016.

[83] H. R. Al Abdallah, "Scholarworks @ UAEU Development of Heat Insulation Composite Materials Based on Bio-Polyesters and Natural Filler," *Theses*, vol. 818, 2021.

[84] J. Lu, D. Wang, P. Jiang, S. Zhang, Z. Chen, and S. Bourbigot, "Design of fire resistant, sound-absorbing and thermal-insulated expandable polystyrene based lightweight particleboard composites," *Construction and Building Materials*, vol. 305, article 124773, 2021.

[85] S. Z. Di Wang, P. Jiang, Z. Chen, J. Sun, H. Li, and X. Gu, "Flame retardant research on innovative lightweight wood-plastic composites," *Journal of Applied Polymer Science*, vol. 140, no. 25, article e53965, 2023.

[86] L. Liu, Y. Xu, Y. He et al., "An effective mono-component intumescent flame retardant for the enhancement of water resistance and fire safety of thermoplastic polyurethane composites," *Polymer Degradation and Stability*, vol. 167, pp. 146–156, 2019.